Toll-Like Receptor 9 Agonists Promote Cellular Invasion by Increasing Matrix Metalloproteinase Activity

Melinda A. Merrell,[1] Joanna M. Ilvesaro,[1] Niko Lehtonen,[5] Timo Sorsa,[5] Bradley Gehrs,[1] Eben Rosenthal,[2] Dongquan Chen,[3] Brit Shackley,[1] Kevin W. Harris,[1,4] and Katri S. Selander[1]

[1]Division of Hematology-Oncology, Department of Medicine, [2]Division of Otolaryngology-Head and Neck Surgery, Department of Surgery, and [3]Biostatistics and Bioinformatics Unit, Comprehensive Cancer Center, University of Alabama at Birmingham; [4]Birmingham Veterans Administration Medical Center, Birmingham, Alabama; and [5]Department of Oral and Maxillofacial Diseases, Institute of Dentistry, University of Helsinki, Helsinki, Finland

Abstract

Toll-like receptor 9 (TLR9) recognizes microbial DNA. We show here that TLR9 protein is expressed in human breast cancer cells and clinical breast cancer samples. Stimulation of TLR9-expressing breast cancer cells with the TLR9 agonistic CpG oligonucleotides (1-10 μmol/L) dramatically increased their *in vitro* invasion in both Matrigel assays and three-dimensional collagen cultures. Similar effects on invasion were seen in TLR9-expressing astrocytoma and glioblastoma cells and in the immortalized human breast epithelial cell line MCF-10A. This effect was not, however, dependent on the CpG content of the TLR9 ligands because the non-CpG oligonucleotides induced invasion of TLR9-expressing cells. CpG or non-CpG oligonucleotide-induced invasion in MDA-MB-231 cells was blunted by chloroquine and they did not induce invasion of TLR9$^-$ breast cancer cells. Treatment of MDA-MB-231 cells with CpG or non-CpG oligonucleotides induced the formation of ~50-kDa gelatinolytic band in zymograms. This band and the increased invasion were abolished by a matrix metalloproteinase (MMP) inhibitor GM6001 but not by a serine proteinase inhibitor aprotinin. Furthermore, CpG oligonucleotide treatment decreased tissue inhibitor of metalloproteinase-3 expression and increased levels of active MMP-13 in TLR9-expressing but not TLR9$^-$ breast cancer cells without affecting MMP-8. Neutralizing anti-MMP-13 antibodies inhibited the CpG oligonucleotide-induced invasion. These findings suggest that infections may promote cancer progression through a novel TLR9-mediated mechanism. They also propose a new molecular target for cancer therapy, because TLR9 has not been associated with cancer invasiveness previously. (Mol Cancer Res 2006;4(7):437–47)

Introduction

Toll-like receptors (TLR) are evolutionarily well-conserved transmembrane proteins that are present in almost all multicellular organisms and recognize patterns specific of microbial components (1, 2). In mammals, the TLR family is currently known to consist of 11 members, which exhibit specificity for pathogen-derived ligands. For example, TLR4 recognizes the bacterial lipopolysaccharide, whereas members of the TLR9 subfamily (TLR7-TLR9) sense the microbial RNA and DNA (1, 2). Oligonucleotides with unmethylated CpG dinucleotides mimic the immunostimulatory activity of bacterial DNA in vertebrates and are also recognized by TLR9 (3-6).

TLR1, TLR2, and TLR4 are expressed on the cell surface, whereas TLR3 and members of the TLR9 subfamily are intracellular (7-10). More specifically, TLR9 is localized to endoplasmic reticulum, from where it is translocated to the endosomal/lysosomal compartment for ligand recognition (10). On ligand binding, the various TLRs and their associated adapters, such as MyD88 and TRIF, recruit intracellular signaling mediators that activate transcription factors, such as nuclear factor-κB. The outcome of TLR activation is an immune reaction characterized by increased production of various proinflammatory cytokines and interleukins (2).

In humans, TLR9 is most abundantly expressed in plasmocytoid dendritic cells and B cells, whereas in mice myeloid dendritic cells as well as macrophages and B cells also express TLR9 (2). Interestingly, several epithelial cell types and astrocytes have also recently been reported to express various TLRs, implying that also other cells than the actual immune cells may be important sentinels of the innate immune system (9, 11-15). High expression of TLR9 was recently detected in

Received 1/10/06; revised 5/15/06; accepted 5/16/06.
Grant support: Department of Defense grant W81XWH-04-1-0600 (K.S. Selander), Academy of Finland (T. Sorsa), and HUCH EVOU TYH 5306, TYH 6104, and TI020Y0002 (T. Sorsa).
The costs of publication of this article were defrayed in part by the payment of page charges. This article must therefore be hereby marked advertisement in accordance with 18 U.S.C. Section 1734 solely to indicate this fact.
Requests for reprints: Katri S. Selander, Division of Hematology-Oncology, Department of Medicine, University of Alabama at Birmingham, WTI T558, 1824 6th Avenue South, Birmingham, AL 35294-3300. Phone: 205-975-5973; Fax: 205-934-9511. E-mail: Katri.Selander@ccc.uab.edu

doi:10.1158/1541-7786.MCR-06-0007

clinical samples of lung cancer and in lung cancer cell lines. In these cells, stimulation of TLR9 with its agonists was shown to result in cytokine production (16). Responsiveness of breast cancer cells to TLR ligands and the presence of TLRs in breast milk suggest that these receptors are also expressed in breast epithelial cells (17, 18).

The aim of this study was to further characterize TLR expression and function in human breast cancer cells. Because the original observation concerning the role of Toll in *Drosophila* was that it mediates dorsoventral patterning, we hypothesized that TLRs may mediate similar functions also in cancer cells (19, 20).

Results

TLR9 Is Expressed in Breast Cancer Cell Lines and Clinical Samples of Breast Cancer

MDA-MB-231 cells express relatively high levels of mRNA for TLR4 and TLR9 but only very little or no mRNA for the other TLR1 to TLR10 as detected in DNA arrays (Fig. 1A). Breast cancer cell responsiveness to lipopolysaccharide, a ligand for TLR4, has been described previously, suggesting that functional TLR4 can be expressed in breast cancer cells (18). Therefore, in this study, we decided to focus on TLR9 expression and function. Flow cytometry as well as immunohistochemistry of the permeabilized MDA-MB-231 cells suggested intracellular expression of TLR9 as also shown previously in other cells (Fig. 1B and C; refs. 2, 21). Anti-TLR9 antibody detected a high level of expression of a band ~120 kDa in MDA-MB-231 cells and an intermediate expression level in T47-D cells, but no specific signal was seen in MCF-7 cells in Western blots (Fig. 1D). TLR9 expression was also detected with Western blot in normal mammary gland tissue and in three of five malignant breast tumors. Interestingly, the TLR9 band detected in the normal mammary gland tissue appeared slightly heavier than the TLR9 band in the malignant tumors and in the MDA-MB-231 cells (Fig. 2A). The same blot was stripped and reblotted with anti-CD45 antibody, which is a pan-leukocyte marker (22). No specific expression of CD45 was seen, suggesting that the TLR9 expression in these lysates is likely from the epithelial cells of the breast (data not shown). TLR9 expression was also detected in immortalized human breast epithelial cell line MCF-10A (Fig. 2B). Taken together, these results suggested that TLR9 is relatively frequently expressed in both normal and cancerous mammary epithelial cells.

TLR9 Agonists Induce Invasion in TLR9-Expressing Cancer Cells

To study the effects of TLR9 stimulation on breast cancer behavior, we did invasion and cell viability assays using the well-characterized TLR9 agonists, CpG motif containing unmethylated oligonucleotides (CpG oligonucleotide), which mimic the actions of bacterial DNA (2). Three different CpG

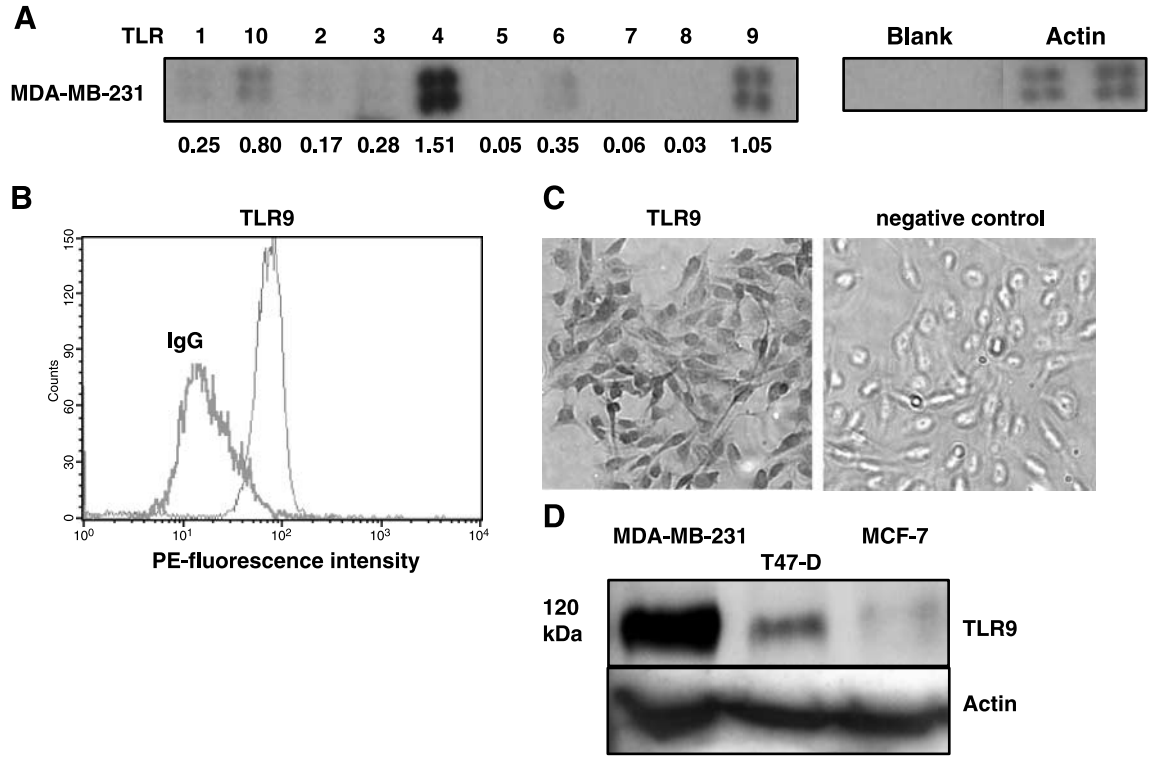

FIGURE 1. Human breast cancer cell lines exhibit different levels of TLR9 expression. **A.** Expression profile of the mRNAs for various TLRs was studied with a DNA array in MDA-MB-231 cells. The calculated numeric levels of expression of each TLR mRNA were obtained after blank subtraction and correction for the expression level of actin. **B.** Specific expression of the TLR9 protein was detected in permeabilized MDA-MB-231 cells using phycoerythrin (PE)–conjugated anti-TLR9 antibody in flow cytometry and (**C**) immunohistochemistry, for which omission of the primary antibody served as a negative control, and (**D**) Western blot detection of the TLR9 protein in the various human breast cancer cells (*top*). The same blots were stripped and reblotted with anti-actin antibodies to show equal loading.

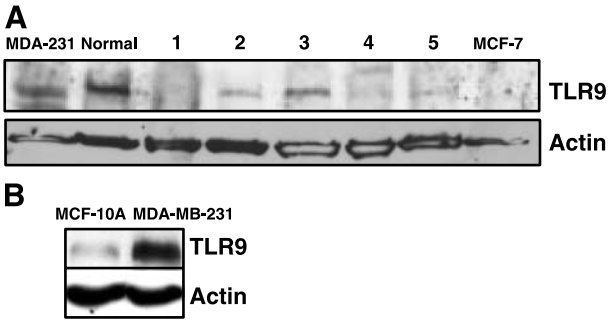

FIGURE 2. TLR9 is expressed in human breast cancer tissues. **A.** Western blot showing the expression of TLR9 in MDA-MB-231 cells and in normal breast tissue obtained at mammoplasty and in breast cancer specimens 1 to 5. **B.** TLR9 expression in immortalized MCF-10A mammary epithelial cells. Both blots were stripped and reblotted with anti-actin antibody to show that the differences in TLR9 expression are not due to unequal loading.

oligonucleotides (types A-C), with slight variations in their sequences, were tested. Types B and C represent CpG oligonucleotides with the conventional nuclease-resistant phosphorothioate backbone, and type A carries a combination of phosphorothioate and phosphodiester modifications. It has been shown previously that such modifications result in a slightly different cytokine responses from dendritic cells at 0.01 to 10 μmol/L concentrations (23). All these CpG oligonucleotides induced a dose-dependent increase in the number of MDA-MB-231 cells that invaded through Matrigel. The treatment-induced increased invasion ranged from 2- to 10-fold and was statistically significant even with the lowest (1 μmol/L) concentrations tested. Surprisingly, the non-CpG oligonucleotides, which are considered unstimulatory controls for the TLR9 agonistic CpG oligonucleotides, induced invasion of MDA-MB-231 cells to a similar level. The type C CpG oligonucleotide was chosen for further studies, because it is a combination of types A and B CpG oligonucleotides and because it induced, along with the type B CpG oligonucleotides, the highest dose responsiveness (Fig. 3A and B). Similar effects on invasion were also seen when MDA-MB-231 cells were cultured for 7 days in the presence of 10 μmol/L type C CpG oligonucleotides in three-dimensional collagen culture assays (Fig. 3C and D). The type C CpG oligonucleotides (10 μmol/L) stimulated invasion also in the unrelated, strongly TLR9-expressing U373 astrocytoma and D54MG glioblastoma cells and in T47-D breast cancer cells (Fig. 3E and F). Treatment with the type C CpG oligonucleotides or with the type C non-CpG oligonucleotides (1 and 10 μmol/L, data not shown for 1 μmol/L) stimulated invasion also in the immortalized mammary epithelial cell line MCF-10A, but they did not, however, stimulate invasion in the TLR9$^-$ MCF-7 breast cancer cells (Fig. 3E and G). The increased cell numbers seen in the invasion assays were not due to an effect on proliferation or apoptosis, because the type C CpG oligonucleotide (10 μmol/L) had no effect on cell viability during an incubation of 24 hours (Fig. 4). During longer incubation (after 3 and 6 days), both type C non-CpG oligonucleotide and type C CpG oligonucleotide actually significantly decreased viability as detected with 3-(4,5-dimethylthiazol-2-yl)-5-(3-carboxymethoxyphenyl)-2-(4-sulfophenyl)-2H-tetrazolium, inner salt assays (Table 1). Taken together, these studies suggested to us that TLR9 agonists stimulate invasion in TLR9$^+$ but not in TLR9$^-$ cancer cells. To further study the role of TLR9 in mediating invasion, we did the invasion assays with and without chloroquine, an inhibitor of endosomal maturation, which has been shown to prevent TLR9 signaling in other cells (24). As shown in Fig. 5, addition of chloroquine (10 μmol/L) inhibited both CpG and non-CpG oligonucleotide-induced invasion. Similar results were obtained also with higher chloroquine doses (25 μmol/L; data not shown), but because they compromised cell viability, they were not routinely used.

TLR9 Agonists Induce Matrix Metalloproteinase Activity

To investigate the mechanism behind the TLR9 agonist-induced invasion, we did gelatin-zymogram assays. Supernatants from MDA-MB-231 cells that were treated with 5 or 10 μmol/L type C CpG oligonucleotides or for 24 hours induced the formation of a gelatinolytic band of ~50 kDa. The appearance of this band was not inhibited with the serine protease inhibitor aprotinin, but it did disappear when the gels were incubated with the broad-spectrum matrix metalloproteinase (MMP) inhibitor GM6001. The size of the band was similar to that induced by a positive MMP-13 control sample (Fig. 6A). Similar results were obtained with the type C non-CpG oligonucleotide (data not shown). Consistent with these findings, the type C CpG-induced invasion of MDA-MB-231 cells was also inhibited by the MMP inhibitor but not by the serine protease inhibitor aprotinin in Matrigel assays (Fig. 6B).

TLR9 Agonist-Induced Invasion Can Be Blocked with Neutralizing Anti-MMP-13 Antibodies

Based on the molecular weight of the CpG oligonucleotide-induced gelatinolytic band, we hypothesized that this treatment induces the activation of MMP-13 (25). ELISA analysis of the supernatants of the MDA-MB-231 breast cancer cells treated with either vehicle or 10 μmol/L type C CpG oligonucleotides indeed revealed significantly increased levels of active MMP-13 in the TLR9 agonist-treated supernatants compared with those of the vehicle-treated cells. Similar induction was seen in the TLR9$^+$ T47-D cells but not in the TLR9$^-$ MCF-7 cells (Fig. 7A). Neutralizing antibodies to MMP-13 also blocked the type C CpG oligonucleotide-induced invasion of MDA-MB-231 and T47-D cells, whereas control antibodies did not (Fig. 7B). Treatment with type C CpG oligonucleotide (10 μmol/L) did not, however, affect the expression of total or active MMP-8 in these cells as judged by Western immunoblotting (Fig. 7C). Specific inhibitor of MMP-8 inhibited basal invasion (mean ± SD number of invaded cells, 50 ± 9 versus 17± 3, basal versus MMP-8 inhibitor, respectively; $P < 0.05$), but it did not block CpG oligonucleotide-induced invasion (Fig. 7D). Taken together, these findings suggested to us that CpG oligonucleotide (and non-CpG oligonucleotide)–induced invasion is mediated via MMP-13. Type C CpG oligonucleotide treatment did not, however, increase MMP-13 expression, suggesting that these TLR9 agonists stimulate breast cancer invasion via activating MMP-13 (Fig. 8A). The TLR9 agonist did not affect the expression of

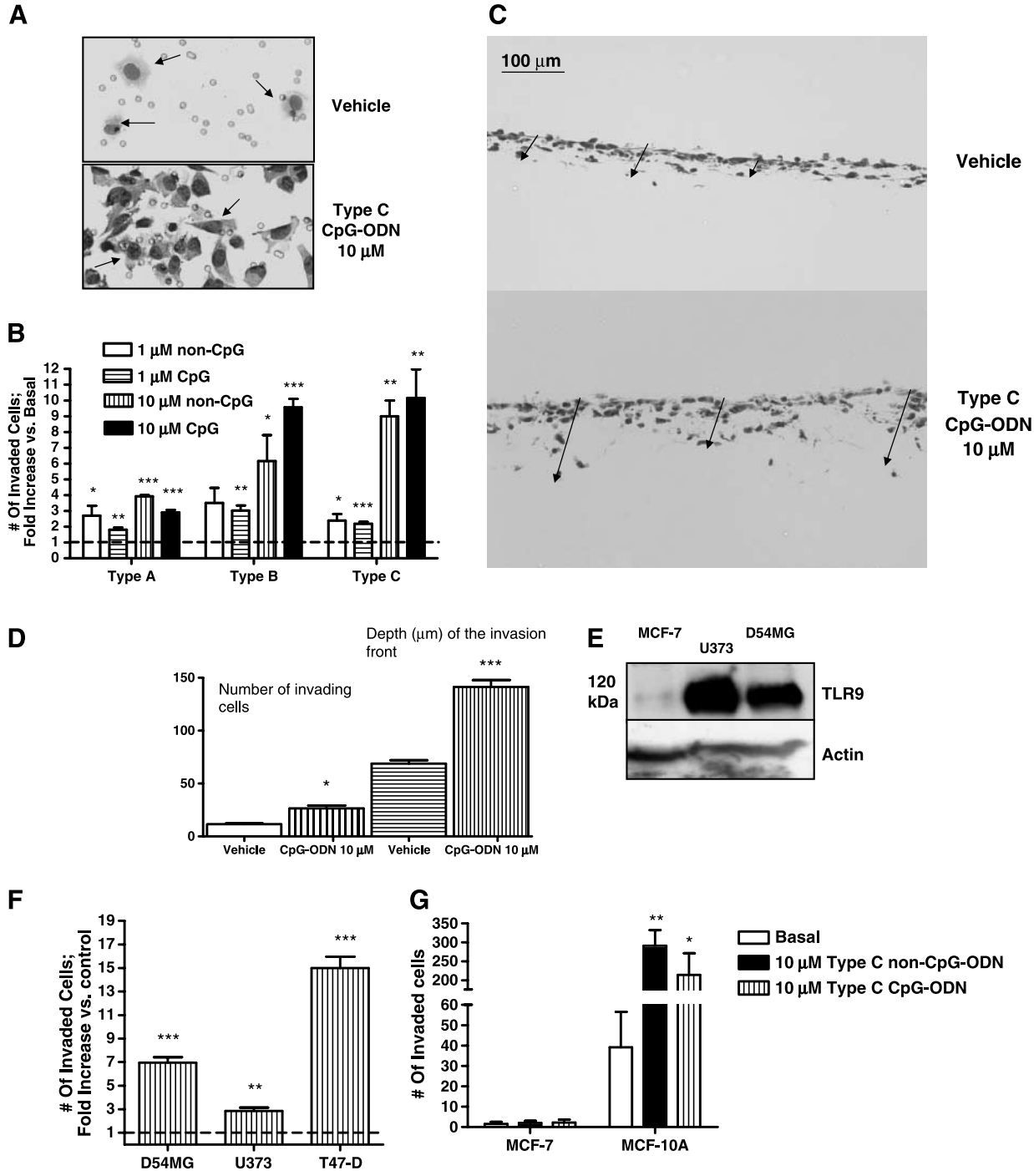

FIGURE 3. TLR9 agonistic CpG oligonucleotides induce invasion of TLR9-expressing cancer cells *in vitro*. **A.** Images of MDA-MB-231 cells (*arrows*) that have invaded through the Matrigel membranes during 18 hours of invasion. **B.** Quantitation of the effects of the various CpG oligonucleotides (ODN) on the invasive capacity of MDA-MB-231 cells were studied in Matrigel assays. Columns, mean fold increase in the number of invaded cells compared with vehicle controls (*dotted line*, set to 1) in each group ($n = 4$); bars, SD. **, $P < 0.01$; ***, $P < 0.001$, versus vehicle. **C.** MDA-MB-231 cells were cultured for 7 days on three-dimensional collagen cultures in the presence of vehicle or 10 μmol/L CpG oligonucleotides. Arrows, front of the invading cells in the gels after they were prepared into H&E-stained histologic samples. **D.** Columns, mean number of invaded cells in the anti-MMP-13 group as a percentage of control in the IgG-treated group. Numbers of invading cells or depths of the invasion front were counted or measured from five representative sites in the cut sections in **C**. The same Y axis scale indicates values for both variables. ($n = 3$); bars, SD. *, $P < 0.05$; ***, $P < 0.001$, versus vehicle. **E.** Western blot detection of the TLR9 protein in U373 astrocytoma and D54MG glioblastoma cells (*top*), where MCF-7 cells represent a negative control. The same blots were stripped and reblotted with anti-actin antibodies (*bottom*) to show equal loading. **F.** Effects of 10 μmol/L type C CpG oligonucleotides on the invasive capacity of the indicated cells were studied in Matrigel assays. Columns, mean fold increase in the number of invaded cells compared with vehicle controls (*dotted line*) in each group ($n = 4$); bars, SD. **, $P < 0.01$; ***, $P < 0.001$, versus vehicle. **G.** Treatment with 10 μmol/L type C CpG oligonucleotides or non-CpG oligonucleotide induced a significant invasion response in the MCF-10A cells, but they had no significant effect on the poorly invasive, TLR9$^-$ MCF-7 breast cancer cells. Columns, mean ($n = 3$-4); bars, SD. *, $P < 0.05$; **, $P < 0.01$, versus basal.

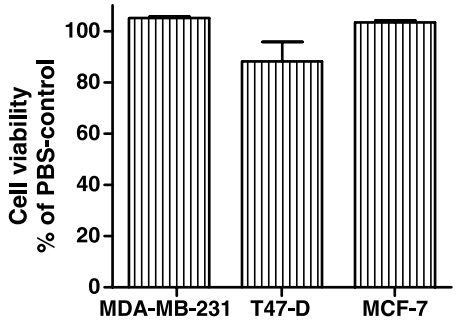

FIGURE 4. Effect on the viability of the indicated breast cancer cells was tested with 3-(4,5-dimethylthiazol-2-yl)-5-(3-carboxymethoxyphenyl)-2-(4-sulfophenyl)-2H-tetrazolium, inner salt assays after treatment for 24 hours with 10 μmol/L type C CpG oligonucleotides or with vehicle. Columns, mean viability as a percentage of vehicle control (n = 4); bars, SD.

plasminogen activator inhibitor-1, plasminogen activator inhibitor-2, or tissue inhibitor of metalloproteinase (TIMP)-1, which can regulate urokinase-type plasminogen activator– and MMP-mediated invasion either (data not shown; refs. 26, 27). We did, however, find differences in the expression levels of TIMP-3, which can inhibit MMP-13 activity (28). Treatment with the type C CpG oligonucleotide decreased the expression of TIMP-3 in the cell lysates of $TLR9^+$ MDA-MB-231 and T47-D cells but not in the $TLR9^-$ MCF-7 cells (Fig. 8B). High levels of TIMP-3, which were not affected by the CpG oligonucleotide treatment, were detected only in the supernatants of the MCF-7 cells.

Discussion

Environmental and epigenetic factors, such as infections and resulting inflammation, are important regulators of tumor progression (29). The innate immune system can promote tumor development and progression through inflammation-dependent mechanisms (29, 30). For example, chemokines and cytokines derived from the immune and inflammatory cells can dramatically affect the host microenvironment and cancer cell behavior, resulting in increased growth and metastasis. Mediators of the innate immunity may also modulate the invasive capacity of cancer cells directly. Endotoxin/lipopolysaccharide, a cell wall constituent of Gram-negative bacteria, has been shown to promote metastasis in a mouse model of colon cancer (31, 32). In addition to the cytokine-mediated indirect effects on tumor progression, lipopolysaccharide-induced effects on metastasis may also be mediated via direct, increased invasiveness of the cancer cells, which frequently express TLRs (32).

We describe here a novel, direct mechanism through which TLR9, a cellular receptor for microbial DNA, may enhance cancer invasiveness. The effects were seen already with 1 μmol/L CpG oligonucleotide, a concentration that induces peak activation of innate immunity in many cellular systems (33-35). Although we used breast cancer cells as a model system, our results imply that a similar mechanism can also be seen in other TLR9-expressing cancers, for example, in brain cancer cells. The fact that expression of TLR9 has also been reported in lung and gastric cancer cells suggests that TLR9-mediated increased invasion may be a general feature in cancer cells that are exposed to infectious agents (9, 15, 16). It was indeed shown recently that also *Helicobacter pylori* induces invasion of gastric cells through TLR2/TLR9-mediated induction of cyclooxygenase-2 (36). The CpG oligonucleotide-induced invasion is not, however, limited to cancer cells alone because we saw similar effects also in the immortalized breast epithelial cell line MCF-10A. In *Drosophila*, Toll was originally identified as a transmembrane receptor required for the establishment of dorsoventral polarity in the developing embryo (20). It was also found to be important in *Drosophila* immunity, as flies lacking this protein were highly susceptible to infection with *Aspergillus fumigatus* (37). Therefore, it seems that both these functions of Toll, the ability to recognize and fight against infectious microorganisms and the ability to mediate invasion, seem evolutionarily well conserved between *Drosophila* and mammalian epithelial cells.

Our findings further suggest that TLR9 agonists stimulate breast cancer invasion via activating MMP-13 but not MMP-8. However, contributions from other MMP family members cannot be ruled out. These findings are in line with the recent reports that showed that in breast cancer cells MMP-8 may actually exert inhibitory effects on invasion (38). The TLR9 agonists did not affect the expression of plasminogen activator inhibitor-1, plasminogen activator inhibitor-2, or TIMP-1, which regulate urokinase-type plasminogen activator– and MMP-mediated invasion either (data not shown; refs. 26, 27). We did, however, discover differences in the expression of TIMP-3, which has been shown to inhibit MMP activity, including MMP-13 (28). CpG oligonucleotide treatment decreased the expression of TIMP-3 in the $TLR9^+$ MDA-MB-231 and T47-D cells but not in the $TLR9^-$ MCF-7 cells. The most prominent effect was seen on the expression of unglycosylated TIMP-3, which has been shown to exhibit similar MMP inhibitory activity than the glycosylated form (39, 40). Interestingly, high levels of TIMP-3 were detected only in the supernatants of the MCF-7 cells, which are poorly invasive. This is surprising in the light that TIMP-3, once

Table 1. CpG or Non-CpG Effect on Long-term Viability

Cells	Day 3			Day 6		
	Vehicle	Non-CpG oligonucleotide	CpG oligonucleotide	Vehicle	Non-CpG oligonucleotide	CpG oligonucleotide
MDA-MB-231	0.358 ± 0.02	0.184 ± 0.002*	0.194 ± 0.008*	1.182 ± 0.03	0.372 ± 0.02*	0.486 ± 0.01*
MCF-7	0.223 ± 0.004	0.166 ± 0.004*	0.166 ± 0.007*	0.418 ± 0.02	0.237 ± 0.02*	0.237 ± 0.008*
T47-D	0.190 ± 0.003	0.089 ± 0.005*	0.084 ± 0.002*	0.419 ± 0.007	0.137 ± 0.005*	0.119 ± 0.004*

NOTE: Cell viability was measured as absorbance at 492 nm (mean ± SD; n = 5).
*P < 0.001 versus vehicle.

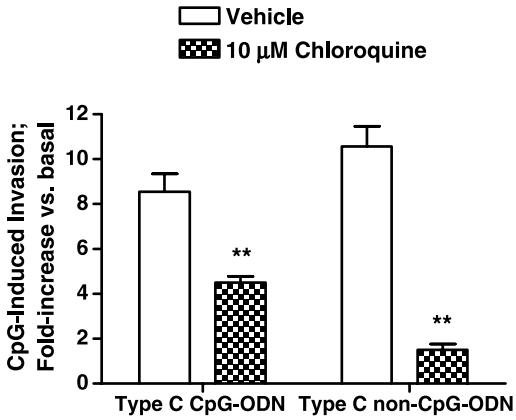

FIGURE 5. CpG oligonucleotide-induced invasion is blocked with chloroquine. MDA-MB-231 cells were allowed to invade through Matrigel membranes for 18 hours in the presence of type C CpG oligonucleotide or non-CpG oligonucleotide (10 μmol/L) with vehicle or chloroquine (10 μmol/L). Columns, mean fold increase in invasion compared with the corresponding unstimulated group ($n = 3$); bars, SD. **, $P < 0.01$, versus vehicle control.

secreted, is typically associated with the insoluble extracellular matrix (39, 41). The reason for this increased localization of TIMP-3 in the MCF-7 supernatants is currently not known, but it may be related to slight differences in protein glycosylation (39). Although the TIMP-3 levels were unaffected by the CpG oligonucleotide treatment in the MCF-7 supernatants, the high constitutive expression of TIMP-3 may partially explain the very low invasive capacity of these cells in general. Taken together, these findings are consistent with our previous report where we showed that increased TIMP-3 expression is associated with decreased invasion in the human MDA-MB-231 breast cancer cells (42). It was also shown previously that treatment of mouse astrocytes with CpG oligonucleotides resulted in increased expression of MMP-9 (4). Therefore, TLR9 agonist-induced MMP profile may be cell specific. Alternatively, the effect in astrocytes may also MMP-13 mediated, because MMP-13 has been shown to activate pro-MMP-9 (43).

It was shown recently that not all CpG oligonucleotide-induced responses are, however, TLR9 mediated. For example, CpG motif containing DNA activated the Akt pathway and this was dependent on the DNA-dependent protein kinase but not on TLR9 (44). Furthermore, plasmid DNA containing CpG motifs elicited similar immune responses in $TLR9^{-/-}$ and in $TLR9^{+/+}$ mice (45). On the other hand, non-CpG oligonucleotides especially in the phosphorothioate backbone induced chemokine induction on the $CD14^{+}$ sorted, $TLR9^{-}$ monocytes, but they did not activate TLR9-transfected cells (34). Non-CpG-containing antisense oligonucleotides activated a proinflammatory response also in TLR9-deficient mice (46). The fact that we saw increased invasion by CpG or non-CpG oligonucleotides and increased MMP-13 activity levels by CpG oligonucleotides only in TLR9-expressing cancer cells but not in $TLR9^{-}$ cells and the fact that the invasion effects of these oligonucleotides were blunted by chloroquine, however, strongly argue that these effects on invasion are mediated via TLR9. This conclusion is supported by a recent report that showed that TLR9 mediates also the effects of non-CpG oligonucleotides, especially if they are phosphorothioate modified (33). Our data, however, imply that TLR9 expression level per se does not correlate with the invasive response to CpG oligonucleotide treatment. This suggest that downstream

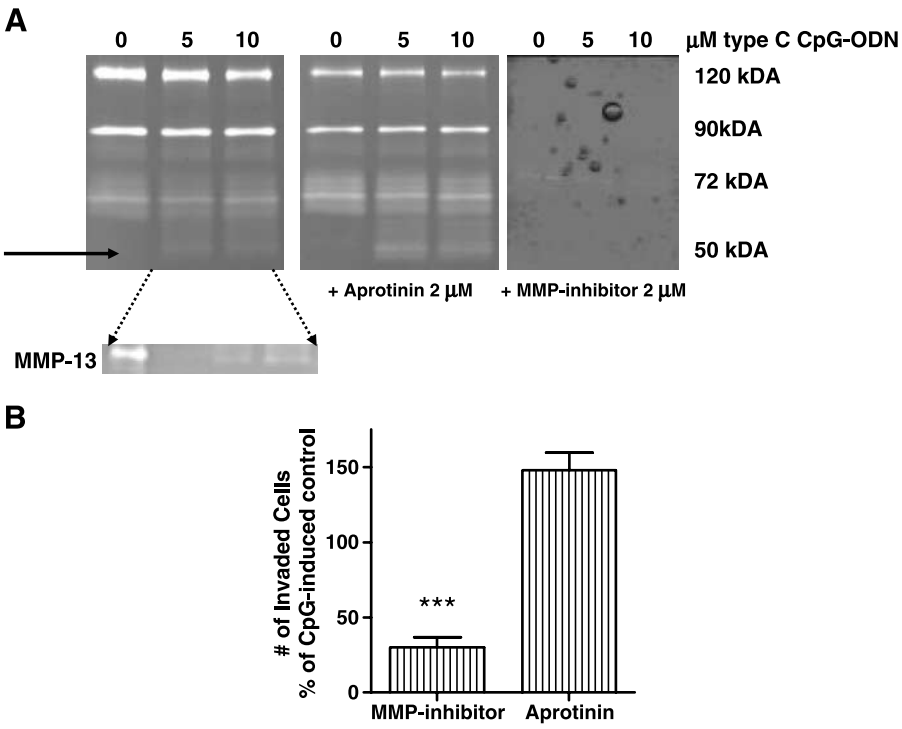

FIGURE 6. CpG oligonucleotide treatment increases MMP activity in MDA-MB-231 cells. **A.** Supernatants from CpG oligonucleotide-treated MDA-MB-231 cells were run on 10% gelatin gels. Treatment with type C CpG oligonucleotides resulted in the appearance of a gelatinolytic band of ~50 kDa (*arrow*), which did not disappear in the presence of aprotinin but was abolished by the addition of a global MMP inhibitor, GM6001, to the final incubation. The formed band was of a similar size than that induced by a positive control for MMP-13 (~50 kDa; *arrows*). **B.** The MMP inhibitor, but not aprotinin (both at 2 μmol/L), inhibited CpG oligonucleotide-induced invasion. Columns, mean number of invaded cells as a percentage of the type C CpG induced (10 μmol/L) control for each group ($n = 3$); bars, SD. ***, $P < 0.001$, versus CpG oligonucleotide treatment alone.

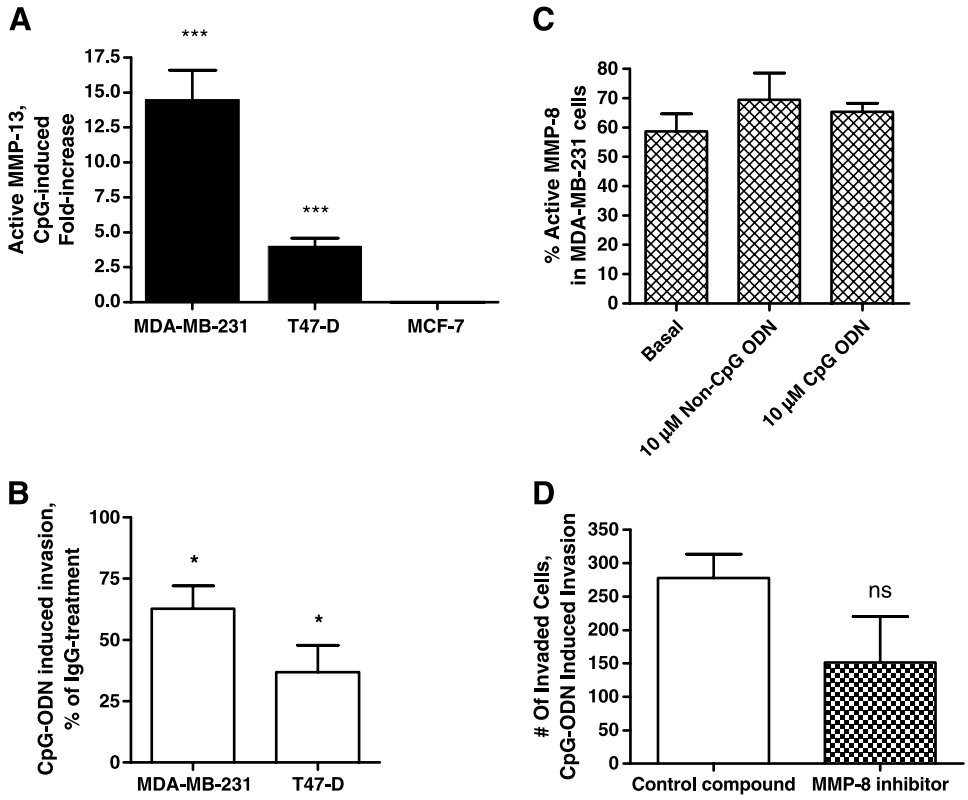

FIGURE 7. CpG oligonucleotide-induced invasion is mediated via MMP-13. **A.** Levels of active MMP-13 from the supernatants of vehicle or type C CpG oligonucleotide-treated (10 μmol/L) in MDA-MB-231, T47-D, and MCF-7 breast cancer cells as analyzed with ELISA. Columns, mean fold increase compared with the vehicle-treated controls for each cell line (n = 3-4); bars, SD. ***, $P < 0.001$, versus vehicle. **B.** Invasive capacity of MDA-MB-231 and T47-D cells was investigated in Matrigels in the presence of 10 μmol/L type C CpG oligonucleotides with neutralizing antibody against MMP-13 or with a control IgG antibody. Columns, mean number of invaded cells in the anti-MMP-13 group as a percentage of control in the IgG-treated group (n = 3); bars, SD. *, $P < 0.05$, versus IgG-treated group. **C.** Percentage of active MMP-8 in MDA-MB-231 cells after treatment with 10 μmol/L type C CpG or non-CpG oligonucleotides. Densitometric analysis of Western blots. **D.** Effects of MMP-8 inhibitor (8 nmol/L) and the same volume of an inactive control compound on type C CpG oligonucleotide-induced invasion of MDA-MB-231 cells in Matrigel assays. Columns, mean (n = 3); bars, SD. No significant differences were found between the two groups.

signaling molecules of the TLR9 pathway may be important regulators of this response. Furthermore, our results suggest that the TLR9 isoform expressed by cancer cells may be different from that expressed in normal mammary epithelial cells. These observations need to be confirmed with further studies.

Our finding has several important implications. First, they may give novel clues to why certain infections; for example, *Mycoplasma* might promote cancer progression (47). *Mycoplasma* infections have been detected in various cancers, including breast cancer (48, 49). After having been taken up by the cells, *Mycoplasma* bacteria have been detected in the same subcellular localization, the lysosome, where also activated TLR9 is localized (21, 50). The identical subcellular location of TLR9 and *Mycoplasma* at least in theory facilitates the possibility that binding of *Mycoplasma* DNA to the cellular TLR9 could result in increased invasion. Second, CpG oligonucleotides are being tested in preclinical models as adjuvants for cancer immunotherapy (51). Although the concentrations of CpGs that have been used to treat mice in the various murine tumor models, where these compounds were shown to have anticancer efficacy possibly through dendritic cell activation, are much lower than the doses used here, our findings warrant caution in the use of immunomodulatory TLR9 agonists in the treatment of cancer and suggest screening of TLR9 expression of the tumors (52, 53). Finally, a recent study revealed a connection between an increased risk for the development of prostate cancer and a sequence variant of TLR4 (54). It is thus possible that similar sequence variations in the TLR9 gene might also explain the individual's susceptibility to cancer progression.

Materials and Methods

Chemicals

Phosphorothioate-modified, human-specific CpG oligonucleotides [type A: 5′-ggGGGACGATCGTCgggggg-3′, in which only the bases that are shown in capital letters are phosphodiester, and those in lower case are phosphorothioate (nuclease resistant), type B: 5′-tcgtcgttttgtcgttttgtcgtt-3′, type C: 5′-tcgtcgtcgttcgaacgacgttgat-3′] and their non-CpG oligonucleotide controls (type A-control: 5′-ggGGGAGCATGCTGgggggc-3′, type B-control: 5′-tgctgcttttgtgcttttgtgctt-3′, type C-control: 5′-tgctgctgcttgcaagcagcttgat-3′) were purchased from Invivogen (San Diego, CA) and dissolved into endotoxin-free sterile distilled H_2O per manufacturer's suggestion and used at the indicated concentrations. Matrigels were from BD

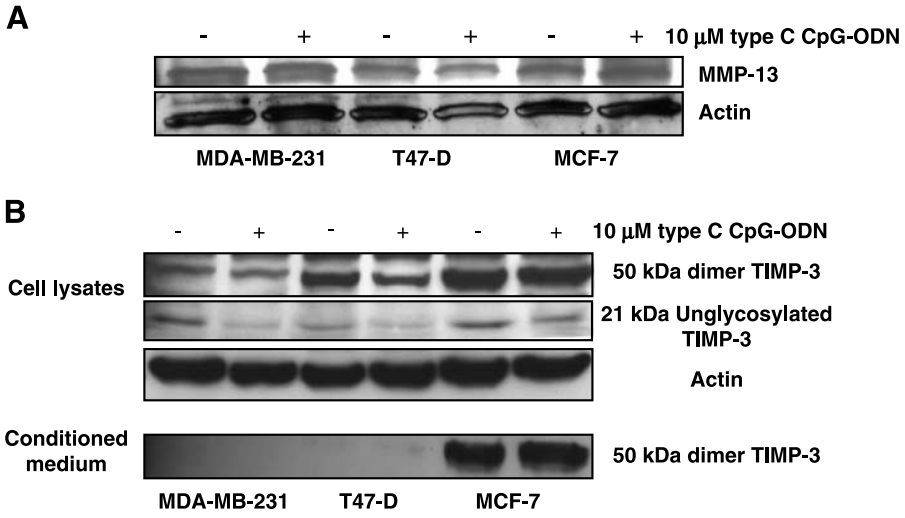

FIGURE 8. A. Western blot of MMP-13 (*top*) in the various breast cancer cell lines with (+) and without (–) 10 μmol/L type C CpG oligonucleotide treatment for 24 hours and after stripping of the same membrane as well as actin expression (*bottom*) to show equal loading. **B.** Western blot of TIMP-3 expression levels from the cell lysates of the indicated breast cancer cells with or without 10 μmol/L type C CpG oligonucleotide treatment for 24 hours. The 50- and 21-kDa bands are from the same blot and represent different TIMP-3 forms. The same blot was stripped and reblotted with anti-actin antibody to show equal loading. Bottom, TIMP-3 expression in cell supernatants from similarly treated cells.

Biosciences (Bedford, MA), serine protease inhibitor aprotinin and MMP inhibitor GM6001 were from EMD Biosciences (La Jolla, CA), MMP-8-specific inhibitor I and the negative control compound were from Calbiochem (San Diego, CA), and MMP-13 immunoblotting standard (human) for the zymography was from Biomol (Plymouth Meeting, PA).

Cell Culture

Human MDA-MB-231 breast cancer, U373 astrocytoma, and D54MG glioblastoma cells were cultured in DMEM (Life Technologies, Paisley, United Kingdom) supplemented with 10% heat-inactivated fetal bovine serum, L-glutamine, penicillin/streptomycin, and nonessential amino acids (all from Life Technologies). T47-D cells were cultured in RPMI, and MCF-7 cells were cultured in α-MEM, supplemented with 10% heat-inactivated FCS, 100 units/mL penicillin, 100 μg/mL streptomycin, and 2 mmol/L glutamine and with 10 μg/mL insulin (Sigma, St. Louis, MO). MCF-10A cells were cultured as described previously in detail (55). All cell cultures were done in incubators in a 37°C atmosphere of 5% CO_2/95% air.

TLR mRNA Expression Profiling

The mRNA expression levels of the various TLRs in MDA-MB-231 cells was investigated using the SuperArray human TLR pathway-specific gene expression profiling system (SuperArray Bioscience Corp., Frederick, MD). Briefly, total cellular RNA was isolated using the RNAzol reagent (Tel-Test, Inc., Friendswood, TX) from the cells grown in normal culture medium and converted to a labeled cDNA probe. The denatured cDNA was hybridized overnight at 60°C to nylon membrane that contained the target cDNAs. Chemiluminescence was used to detect the hybridization signal on a X-ray film (Eastman Kodak Co., Rochester, NY). Per manufacturer's instructions, the X-ray film was scanned with a high-resolution scanner (~300 dpi) into a JPEG-format image and converted into a TIFF format (8-bit inverted grayscale) image by using a Photoshop software (Adobe Systems, Inc., San Jose, CA). The images were then uploaded into a software ScanAlyze (Eisen Lab, University of California at Berkeley) to produce a raw intensity data sheet. The raw data from both the control and the treated groups were combined and uploaded into a software GEarray Analyzer (SuperArray, Inc., Bethesda, MD), where differences and ratios between the treated and the control groups were analyzed. Background was subtracted from signals and a housekeeping gene, such as actin, was used to calculate the ratio.

Flow Cytometry

MDA-MB-231 cells were cultured on Petri dish (Ø 15 cm) until ~70% confluent. The cells were then detached using CellStripper (Fisher Scientific, Hampton, NH) and prepared for analysis using the BD Cytofix/Cytoperm kit (BD Biosciences, San Diego, CA) according to the manufacturer's recommendations. Briefly, ~1×10^6 cells were suspended into 0.5 mL of the fixative solution. After washing the cells twice, phycoerythrin-conjugated anti-human TLR9 antibody (eBioscience, San Diego, CA) or phycoerythrin-conjugated, isotype-controlled IgG was added to the cells (7 μL/tube). After incubation for 30 minutes at 4°C, the cells were rinsed twice with PBS and analyzed with fluorescence-activated cell sorting.

Immunohistochemistry

For the immunohistochemical stainings, the MDA-MB-231 cells were grown on glass coverslips in normal culture medium. The cells were fixed with 3% paraformaldehyde-PBS for 10 minutes at room temperature, after which they were permeabilized with 0.025% saponin for 30 minutes on ice. After blocking the samples with 10% goat serum, staining with mouse monoclonal antibody to TLR9 (Abcam, Inc., Cambridge, MA) was done. Horseradish peroxidase–conjugated anti-mouse antibody was used to visualize the staining. The samples were then examined using a Leica (Bannockburn, IL) light microscope.

Western Blotting

The cells were cultured on six-well plates in their normal culture medium until near confluency, after which they were rinsed with sterile PBS and cultured for further 24 hours in serum-free culture medium. The culture medium was then

discarded and the cells were harvested in lysis buffer [20 mmol/L Tris (pH 7.4), 150 mmol/L NaCl, 1 mmol/L EDTA, 1 mmol/L EGTA, 1% Triton, 2.5 mmol/L sodium pyrophosphate, 1 mmol/L β-glycerophosphate, 1 mmol/L Na_3VO_4, 1 μg/mL leupeptin; Cell Signaling, Beverly, MA] and clarified by centrifugation. After boiling the supernatants in reducing SDS sample buffer for 5 minutes, equal amounts of protein (~50 μg) were loaded per lane and the samples were electrophoresed on 10% polyacrylamide SDS gel and transferred to a nitrocellulose membrane. TLR9 and TIMP-3 were detected with anti-TLR9 (IMG-431; Imgenex, San Diego, CA) and anti-human TIMP-3 (AB802; Chemicon International, Temecula, CA) antibodies. MMP-13 was detected with anti-human MMP-13 antibody (R&D Systems, Minneapolis, MN). Binding of the primary antibodies to the target proteins on the membranes was revealed with species-specific horseradish peroxidase–conjugated secondary antibodies (Cell Signaling). The same blots were stripped and reblotted, using anti-actin antibody (Sigma), to show equal loading. The protein bands were visualized by chemiluminescence using SuperSignal West Pico Enhanced Chemiluminescence kit (Pierce, Rockford, IL). Expression of TLR9 in human breast cancer specimens or normal breast tissue was studied from specimens that were obtained from the University of Alabama at Birmingham tissue repository. Briefly, the tissues were homogenized in the lysis buffer and analyzed with Western blotting as described above. The use of these samples for this purpose was accepted by the local institutional review board.

In vitro *Invasion Assays*

For the Matrigel invasion assay, the cells were plated at the density of 5×10^4 (MDA-MB-231, U373, and D54MG), 15×10^4 (T47-D), or 30×10^4 (MCF-7) per upper well in 750 μL normal culture medium (56). Indicated concentrations of the various CpG oligonucleotides, non-CpG oligonucleotides, or vehicle were added to both upper and lower wells. When indicated, aprotinin (2 μmol/L), GM6001 (2 μmol/L), MMP-8 inhibitor I (8 nmol/L), or the same volume of the corresponding control compound, control IgG or neutralizing anti-MMP-13 antibody (R&D Systems; both at 12 μg/mL) or chloroquine (10 μmol/L) were also added to both upper and lower wells. The cells were allowed to invade for 18 hours, after which the inserts were removed and stained with the Hema 3 Stain set (Fisher Diagnostics, Middletown, PA) according to the manufacturer's recommendation. The number of invaded cells were counted from five preselected microscopic fields using a ×40 objective. To assess invasion in a three-dimensional type I collagen gel, acid-solubilized type I collagen (0.9 ml) was added to the Costar Transwell dishes (Corning, Inc., Corning, NY) and gelled over 45 minutes at 37°C. The collagen was prepared using rat tail type I collagen dissolved in 0.2% acetic acid at 3.2 mg/mL and gelled by neutralizing the acid with 0.3 N NaOH containing phenol red as a pH indicator. A final concentration of 3.0 mg/mL was obtained. Medium containing vehicle or 10 μmol/L type C CpG oligonucleotide was then added to the upper and lower chambers before the addition of 5×10^5 cells to the surface of the collagen gel in the presence of serum-containing medium. Medium was changed every 3 days over the 7-day incubation period. Gels were then removed from the Transwell dish, fixed in 2.7% formaldehyde for 24 hours, and embedded in paraffin. Sections (6 μm) were cut and stained with H&E. Tumor cell invasion (depth and number of cells below the surface) was assessed by light microscopy in a minimum of four randomly selected sections for each experimental sample. The number of invading cells per high-power field (×400) was counted and averaged. The depth of invasion was also measured in four randomly selected areas for each sample using photomicrograph of each sample.

Cell Viability Assays

MDA-MB-231, T47-D, or MCF-7 cells were plated at the density of 1,000 per well in 96-well plates in normal culture medium and cultured for the indicated periods of time with 10 μmol/L type C CpG oligonucleotide or vehicle. Cell viability was assessed after 3-(4,5-dimethylthiazol-2-yl)-5-(3-carboxymethoxyphenyl)-2-(4-sulfophenyl)-2H-tetrazolium, inner salt was added for the final 2 hours of the experimental cultures as recommended by the manufacturer (CellTiter 96 AQ_{ueous} Nonradioactive Cell Proliferation Assay, Promega, Madison, WI).

Zymograms

The zymograms were done as described previously (57). In this assay, the gelatinolytic bands represent the following MMPs: 120-kDa band represents MMP-9 and neutrophil gelatinase-associated lipocalin complex, 90-kDa band represents pro-MMP-9, and the 72-kDa band represents pro-MMP-2 (58-60). Briefly, MDA-MB-231 cells were plated on 12-well plates and allowed to reach confluency. The cells were then rinsed with PBS and serum-free medium, with the indicated concentrations of type C CpG oligonucleotides, type C non-CpG oligonucleotides, or vehicle applied for 24 hours. The supernatants were then collected and a 35 μL aliquot was applied to zymograms (Novex 10% gelatin gels, Invitrogen, Carlsbad, CA) according to the manufacturer's suggestions. In further experiments, aprotinin (2 μmol/L) or GM6001 (2 μmol/L) was added to the final incubations of the gels to investigate whether CpG treatment induced serine protease or MMP activity.

MMP-13 ELISA

MDA-MB-231, T47-D, and MCF-7 cells were plated on 24-well plates at the density of 10^5 per well and allowed to reach confluency. The cells were then rinsed with PBS, and 200 μL serum-free medium, containing vehicle or 10 μmol/L type C CpG oligonucleotides, was added per well. The supernatants were collected 24 hours later and analyzed for levels of active MMP-13 with an ELISA that detects active MMP-13 (Calbiochem, La Jolla, CA) according to the manufacturer's instructions.

MMP-8 Analysis

The molecular forms and degree of activation of MMP-8 were analyzed by Western immunoblotting using anti-rabbit MMP-8 antibody (61). After SDS-PAGE run under nonreducing conditions, the proteins on the gel were transferred onto a nitrocellulose filter (Bio-Rad Laboratories, Richmond, CA).

After blocking with 3% gelatin, the membrane first reacted with the primary antibody (1:500) and then with alkaline phosphatase–conjugated secondary antibody. Immunoreactive proteins were visualized by nitroblue tetrazolium (Sigma) and 5-bromo-4-chloro-3-indolyl-phosphate (Sigma). Quantitation was done with the Bio-Rad imaging densitometer using the Analyst program. Data are expressed as densitometric arbitrary units. Human neutrophil and rheumatoid synovial culture medium were used as positive controls for polymorphonuclear-type and mesenchymal-type MMP-8 isoforms, respectively (62).

Statistical Analysis

Results are mean ± SD unless otherwise stated. Student's *t* test was used to calculate statistically significant differences between the various study groups.

Acknowledgments

We thank Telisha Millender-Swain and Wenyue Zhang for skilled technical help and Dr. Theresa Strong for providing the clinical breast cancer lysates.

References

1. Akira S, Hemmi H. Recognition of pathogen-associated molecular patterns by TLR family. Immunol Lett 2003;85:85–95.

2. Wagner H. The immunobiology of the TLR9 subfamily. Trends Immunol 2004;25:381–6.

3. Hemmi H, Takeuchi O, Kawai T, et al. A Toll-like receptor recognizes bacterial DNA. Nature 2000;408:740–5.

4. Lee S, Hong J, Choi SY, et al. CpG oligodeoxynucleotides induce expression of proinflammatory cytokines and chemokines in astrocytes: the role of c-Jun N-terminal kinase in CpG ODN-mediated NF-κB activation. J Neuroimmunol 2004;153:50–63.

5. Latz E, Visintin A, Espevik T, Golenbock DT. Mechanisms of TLR9 activation. J Endotoxin Res 2004;10:406–12.

6. Takeshita F, Gursel I, Ishii KJ, Suzuki K, Gursel M, Klinman DM. Signal transduction pathways mediated by the interaction of CpG DNA with Toll-like receptor 9. Semin Immunol 2004;16:17–22.

7. Matsumoto M, Funami K, Tanabe M, et al. Subcellular localization of Toll-like receptor 3 in human dendritic cells. J Immunol 2003;171:3154–62.

8. Nishiya T, DeFranco AL. Ligand-regulated chimeric receptor approach reveals distinctive subcellular localization and signaling properties of the Toll-like receptors. J Biol Chem 2004;279:19008–17.

9. Schmausser B, Andrulis M, Endrich S, et al. Expression and subcellular distribution of toll-like receptors TLR4, TLR5 and TLR9 on the gastric epithelium in *Helicobacter pylori* infection. Clin Exp Immunol 2004;136:521–6.

10. Leifer CA, Kennedy MN, Mazzoni A, Lee C, Kruhlak MJ, Segal DM. TLR9 is localized in the endoplasmic reticulum prior to stimulation. J Immunol 2004; 173:1179–83.

11. Schaefer TM, Desouza K, Fahey JV, Beagley KW, Wira CR. Toll-like receptor (TLR) expression and TLR-mediated cytokine/chemokine production by human uterine epithelial cells. Immunology 2004;112:428–36.

12. Bowman CC, Rasley A, Tranguch SL, Marriott I. Cultured astrocytes express toll-like receptors for bacterial products. Glia 2003;43:281–91.

13. Platz J, Beisswenger C, Dalpke A, et al. Microbial DNA induces a host defense reaction of human respiratory epithelial cells. J Immunol 2004;173: 1219–23.

14. Mempel M, Voelcker V, Kollisch G, et al. Toll-like receptor expression in human keratinocytes: nuclear factor κB controlled gene activation by *Staphylococcus aureus* is toll-like receptor 2 but not toll-like receptor 4 or platelet activating factor receptor dependent. J Invest Dermatol 2003;121:1389–96.

15. Schmausser B, Andrulis M, Endrich S, Muller-Hermelink HK, Eck M. Toll-like receptors TLR4, TLR5 and TLR9 on gastric carcinoma cells: an implication for interaction with *Helicobacter pylori*. Int J Med Microbiol 2005;295:179–85.

16. Droemann D, Albrecht D, Gerdes J, et al. Human lung cancer cells express functionally active Toll-like receptor 9. Respir Res 2005;6:1.

17. LeBouder E, Rey-Nores JE, Rushmere NK, et al. Soluble forms of Toll-like receptor (TLR) 2 capable of modulating TLR2 signaling are present in human plasma and breast milk. J Immunol 2003;171:6680–9.

18. Zaks-Zilberman M, Zaks TZ, Vogel SN. Induction of proinflammatory and chemokine genes by lipopolysaccharide and paclitaxel (Taxol) in murine and human breast cancer cell lines. Cytokine 2001;15:156–65.

19. Parker JS, Mizuguchi K, Gay NJ. A family of proteins related to Spatzle, the toll receptor ligand, are encoded in the *Drosophila* genome. Proteins 2001;45: 71–80.

20. Hashimoto C, Hudson KL, Anderson KV. The Toll gene of *Drosophila*, required for dorsal-ventral embryonic polarity, appears to encode a transmembrane protein. Cell 1988;52:269–79.

21. Latz E, Schoenemeyer A, Visintin A, et al. TLR9 signals after translocating from the ER to CpG DNA in the lysosome. Nat Immunol 2004;5:190–8.

22. Xu Y, Harder KW, Huntington ND, Hibbs ML, Tarlinton DM. Lyn tyrosine kinase: accentuating the positive and the negative. Immunity 2005;22:9–18.

23. Hemmi H, Kaisho T, Takeda K, Akira S. The roles of Toll-like receptor 9, MyD88, and DNA-dependent protein kinase catalytic subunit in the effects of two distinct CpG DNAs on dendritic cell subsets. J Immunol 2003;170:3059–64.

24. Rutz M, Metzger J, Gellert T, et al. Toll-like receptor 9 binds single-stranded CpG-DNA in a sequence- and pH-dependent manner. Eur J Immunol 2004;34: 2541–50.

25. Freije JM, Diez-Itza I, Balbin M, et al. Molecular cloning and expression of collagenase-3, a novel human matrix metalloproteinase produced by breast carcinomas. J Biol Chem 1994;269:16766–73.

26. Morgan H, Hill PA. Human breast cancer cell-mediated bone collagen degradation requires plasminogen activation and matrix metalloproteinase activity. Cancer Cell Int 2005;5:1.

27. Cakarovski K, Leung JY, Restall C, et al. Novel inhibitors of urokinase-type plasminogen activator and matrix metalloproteinase expression in metastatic cancer cell lines. Int J Cancer 2004;110:610–6.

28. Ala-Aho R, Johansson N, Baker AH, Kähäri VM. Expression of collagenase-3 (MMP-13) enhances invasion of human fibrosarcoma HT-1080 cells. Int J Cancer 2002;97:283–9.

29. Coussens LM, Werb Z. Inflammation and cancer. Nature 2002;420:860–7.

30. Coussens LM, Werb Z. Inflammatory cells and cancer: think different! J Exp Med 2001;193:F23–6.

31. Pidgeon GP, Harmey JH, Kay E, Da Costa M, Redmond HP, Bouchier-Hayes DJ. The role of endotoxin/lipopolysaccharide in surgically induced tumour growth in a murine model of metastatic disease. Br J Cancer 1999;81:1311–7.

32. Harmey JH, Bucana CD, Lu W, et al. Lipopolysaccharide-induced metastatic growth is associated with increased angiogenesis, vascular permeability and tumor cell invasion. Int J Cancer 2002;101:415–22.

33. Roberts TL, Sweet MJ, Hume DA, Stacey KJ. Cutting edge: species-specific TLR9-mediated recognition of CpG and non-CpG phosphorothioate-modified oligonucleotides. J Immunol 2005;174:605–8.

34. Bartz H, Mendoza Y, Gebker M, Fischborn T, Heeg K, Dalpke A. Polyguanosine strings improve cellular uptake and stimulatory activity of phosphodiester CpG oligonucleotides in human leukocytes. Vaccine 2004;23:148–55.

35. Roberts TL, Dunn JA, Terry TD, et al. Differences in macrophage activation by bacterial DNA and CpG-containing oligonucleotides. J Immunol 2005;175: 3569–76.

36. Chang YJ, Wu MS, Lin JT, Chen CC. *Helicobacter pylori*-induced invasion and angiogenesis of gastric cells is mediated by cyclooxygenase-2 induction through TLR2/TLR9 and promoter regulation. J Immunol 2005;175:8242–52.

37. Lemaitre B, Nicolas E, Michaut L, Reichhart JM, Hoffmann JA. The dorsoventral regulatory gene cassette Spatzle/Toll/cactus controls the potent antifungal response in *Drosophila* adults. Cell 1996;86:973–83.

38. Montel V, Kleeman J, Agarwal D, Spinella D, Kawai K, Tarin D. Altered metastatic behavior of human breast cancer cells after experimental manipulation of matrix metalloproteinase 8 gene expression. Cancer Res 2004;64:1687–94.

39. Langton KP, Barker MD, McKie N. Localization of the functional domains of human tissue inhibitor of metalloproteinases-3 and the effects of a Sorsby's fundus dystrophy mutation. J Biol Chem 1998;273:16778–81.

40. Stricklin GP. Human fibroblast tissue inhibitor of metalloproteinases: glycosylation and function. Coll Relat Res 1986;6:219–28.

41. Leco KJ, Khokha R, Pavloff N, Hawkes SP, Edwards DR. Tissue inhibitor of metalloproteinases-3 (TIMP-3) is an extracellular matrix-associated protein with a distinctive pattern of expression in mouse cells and tissues. J Biol Chem 1994; 269:9352–60.

42. Selander KS, Li L, Watson L, et al. Inhibition of gp130 signaling in breast cancer blocks constitutive activation of Stat3 and inhibits *in vivo* malignancy. Cancer Res 2004;64:6924–33.

43. Knauper V, Smith B, Lopez-Otin C, Murphy G. Activation of progelatinase B

(proMMP-9) by active collagenase-3 (MMP-13). Eur J Biochem 1997;248: 369–73.

44. Dragoi AM, Fu X, Ivanov S, et al. DNA-PKcs, but not TLR9, is required for activation of Akt by CpG-DNA. EMBO J 2005;24:779–89.

45. Babiuk S, Mookherjee N, Pontarollo R, et al. $TLR9^{-/-}$ and $TLR9^{+/+}$ mice display similar immune responses to a DNA vaccine. Immunology 2004;113: 114–20.

46. Senn JJ, Burel S, Henry SP. Non-CpG-containing antisense 2′-methoxyethyl oligonucleotides activate a proinflammatory response independent of Toll-like receptor 9 or myeloid differentiation factor 88. J Pharmacol Exp Ther 2005;314: 972–9.

47. Cimolai N. Do mycoplasmas cause human cancer? Can J Microbiol 2001;47: 691–7.

48. Huang S, Li JY, Wu J, Meng L, Shou CC. *Mycoplasma* infections and different human carcinomas. World J Gastroenterol 2001;7:266–9.

49. Pehlivan M, Itirli G, Onay H, Bulut H, Koyuncuoglu M, Pehlivan S. Does *Mycoplasma* sp. play role in small cell lung cancer? Lung Cancer 2004;45:129–30.

50. Yavlovich A, Tarshis M, Rottem S. Internalization and intracellular survival of *Mycoplasma pneumoniae* by non-phagocytic cells. FEMS Microbiol Lett 2004;233:241–6.

51. Wooldridge JE, Weiner GJ. CpG DNA and cancer immunotherapy: orchestrating the antitumor immune response. Curr Opin Oncol 2003;15:440–5.

52. Meng Y, Carpentier AF, Chen L, et al. Successful combination of local CpG-ODN and radiotherapy in malignant glioma. Int J Cancer 2005;116:992–7.

53. Ninalga C, Loskog A, Klevenfeldt M, Essand M, Totterman TH. CpG oligonucleotide therapy cures subcutaneous and orthotopic tumors and evokes protective immunity in murine bladder cancer. J Immunother 2005;28:20–7.

54. Zheng SL, Augustsson-Balter K, Chang B, et al. Sequence variants of Toll-like receptor 4 are associated with prostate cancer risk: results from the Cancer Prostate in Sweden Study. Cancer Res 2004;64:2918–22.

55. Debnath J, Muthuswamy SK, Brugge JS. Morphogenesis and oncogenesis of MCF-10A mammary epithelial acini grown in three-dimensional basement membrane cultures. Methods 2003;30:256–68.

56. Virtanen SS, Väänänen HK, Härkönen PL, Lakkakorpi PT. Alendronate inhibits invasion of PC-3 prostate cancer cells by affecting the mevalonate pathway. Cancer Res 2002;62:2708–14.

57. Suarez-Cuervo C, Merrell MA, Watson L, et al. Breast cancer cells with inhibition of p38α have decreased MMP-9 activity and exhibit decreased bone metastasis in mice. Clin Exp Metastasis 2004;21:525–33.

58. Sorsa T, Salo T, Koivunen E, et al. Activation of type IV procollagenases by human tumor-associated trypsin-2. J Biol Chem 1997;272:21067–74.

59. Kjeldsen L, Johnsen AH, Sengelov H, Borregaard N. Isolation and primary structure of NGAL, a novel protein associated with human neutrophil gelatinase. J Biol Chem 1993;268:10425–32.

60. Westerlund U, Ingman T, Lukinmaa PL, et al. Human neutrophil gelatinase and associated lipocalin in adult and localized juvenile periodontitis. J Dent Res 1996;75:1553–63.

61. Prikk K, Maisi P, Pirila E, et al. Airway obstruction correlates with collagenase-2 (MMP-8) expression and activation in bronchial asthma. Lab Invest 2002;82:1535–45.

62. Hanemaaijer R, Sorsa T, Konttinen YT, et al. Matrix metalloproteinase-8 is expressed in rheumatoid synovial fibroblasts and endothelial cells. Regulation by tumor necrosis factor-α and doxycycline. J Biol Chem 1997;272: 31504–9.